16th World Conference on Earthquake Engineering, 16WCEE 2017
Santiago Chile, January 9th to 13th 2017
Paper N° 1325
Registration Code: S-V1464648321

METHODOLOGY BASED ON CONDITIONAL SCENARIO SPECTRA TO ESTIMATE ENGINEERING DEMAND PARAMETER RISK

C.A. Arteta[1], N. Abrahamson[2]

(1) Assistant Professor, Dept. of Civil and Environmental Engineering, Universidad del Norte, Barranquilla, Colombia, carteta@uninorte.edu.co
(2) Professor, Dept. of Civil and Environmental Engineering, University of California, Berkeley, abrahamson@berkeley.edu.

Abstract

Earthquake risk reduction requires robust analysis frameworks to estimate the vulnerability of structural systems subjected to seismic shaking. A methodology to estimate risk of structural response quantities such as maximum story drift ratio, maximum base shear or collapse is presented. The risk is calculated by means of nonlinear dynamic analysis, using a large suite of ground motions selected and scaled based on the so-called Conditional Scenario Spectra (CSS). The CSS are a set of realistic earthquake spectra with assigned rates of occurrence that reproduce the hazard at a site over 10-2 to 10-5 annual exceedance for periods of 0.1 to 4 seconds. The set of ground motion is thought to represent the seismic history of the site over a few thousand years, and allows estimating the return period of engineering demand parameters (EDP) to evaluate their acceptability. The methodology also serves as an objective platform to compare the seismic response of structural systems. As an example to the methodology, the seismic risk of EDPs of a ductile and a nonductile reinforced concrete shear wall are presented.

Keywords: engineering demand parameter, risk, Conditional Scenario Spectra, hazard consistent structural response.

1. Introduction

Seismic vulnerability assessment requires a robust analysis framework that allows evaluating demand parameters with a hazard-consistent basis. Seismic structural response evaluations are typically performed in engineering offices using a small suite of recorded ground motions. These recordings are scaled or modified to fit certain target demand criteria such as ground motion intensity levels and/or frequency content. The ground motion selection process is routinely based on the probable seismic scenario that may affect the structure in consideration. This is done by selecting trios of magnitude, distance, and site conditions from a hazard deaggregation. Selected candidate accelerograms have properties near the target value, and structural analyses with a small set of accelerograms are usually performed with 3 to 11 sets of 1-, 2-, or 3-component ground motions. This is appropriate if the objective is the median response, but it is not if the objective is also estimating the variability of the demand on the structural system. To estimate the variability in structural responses, other approaches use large sets of records that test the behaviour of the structural model over a large range of ground motion intensities. One such approach is the Incremental Dynamic Analysis (IDA) [1]. This analysis methodology uses a set of seed ground motions which are scaled progressively to perform response history analyses of the structural model in consideration. Per scaling factor, each ground motion has an associated intensity value (for example, spectral acceleration at the fundamental structural period, Sa(T1)), and a corresponding peak structural response of interest. The ground motions scaling factor are incremented until a response threshold is surpassed for each ground motion. At the end of the analysis process, each EDP level of interest is associated to a distribution of intensity values. Figure 1 shows an example of the IDA results along with the estimation of two points of a corresponding fragility curve, which effectively accounts for the structural response variability and provides the probability of surpassing certain EDP level given specific intensity values (Sa(T1)) occur. A main disadvantage of the IDA methodology is that the structural responses will vary depending on the seed ground motions used. Also, the scaling factors used to increase the intensity of each ground motion may produce unrealistic spectral shapes because the shapes are constant, but they should depend on the hazard level (e.g., spectra are more peaked at the low probability levels). This may produce unlikely structural responses that are not necessarily consistent with the estimated hazard.

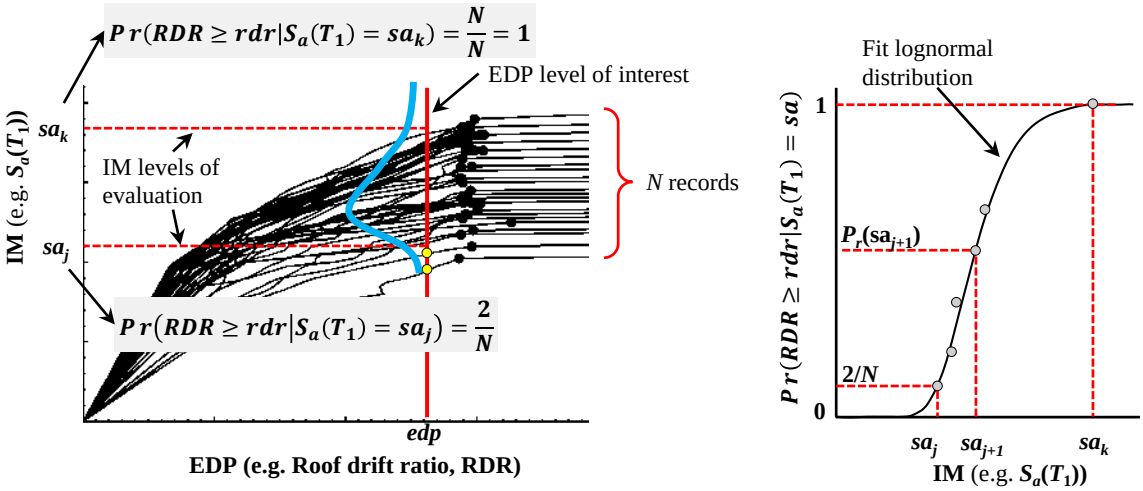

Figure 1 – IDA results and corresponding fragility curve estimation (adapted from Haindl et al [2])

This article presents a methodology based on the Conditional Scenario Spectra (CSS) to estimate the risk of structural response quantities (or EDPs). The CSS are a set of realistic earthquake spectra with assigned rates of occurrence that reproduce the hazard at a site over 10-2 to 10-5 annual exceedance for periods of 0.1 to 4 seconds. The set of ground motion is thought to represent the seismic history of the site over 10,000 years, and allows estimating the return period of EDPs to evaluate their acceptability. A numerical example of a prototype code-compliant special structural wall under seismic shaking is presented to show an implementation of this hazard-consistent response assessment methodology. The impact of the reinforced concrete material behaviour is

discussed in terms of the resulting risk of the roof drift ratio (RDR) and the maximum compressive strain demand at the edge of the wall.

2. Conditional scenario spectra (CSS) for EDP risk estimation

Engineering demand parameters (EDP) may comprise structural responses at the global level such as maximum story drift, base shear force, and partial or total collapse, as well as responses at the local structural level such as the uniaxial strain demand at the critical section a structural wall. The EDP risk is estimated by means of nonlinear dynamic analyses under a large suite of ground motions selected and scaled based on the so-called Conditional Spectra (CS) [3,4]. The Conditional Scenario Spectra (CSS) are a set of realistic earthquake spectra with assigned rates of occurrence based on their spectral shape and intensity. To ensure that each spectrum has the correct shape, the CSS ground motion selection procedure makes use of estimated Conditional Mean Spectra (CMS) [5], anchored at a conditioning period, at different hazard levels. Given the occurrence of the spectral acceleration of a UHS at a conditioning period, the CMS provides the geometric mean response spectrum at all periods of interest. Ground motion time series are selected based on the hazard deaggregation at the site, and are scaled to account for the peak and trough variability around a CMS at various hazard levels. The initial assigned rate of occurrence for each time series is based on the hazard level of the Uniform Hazard Spectrum (UHS) at the conditioning period of the aforementioned CMS. The assigned rates to each time series are then numerically optimized such that their calculated hazard matches the target hazard curves for a range of hazard levels and frequencies of interest. Figure 2 presents the set of 402 ground motion spectra used for this study along with their final assigned rates of occurrence

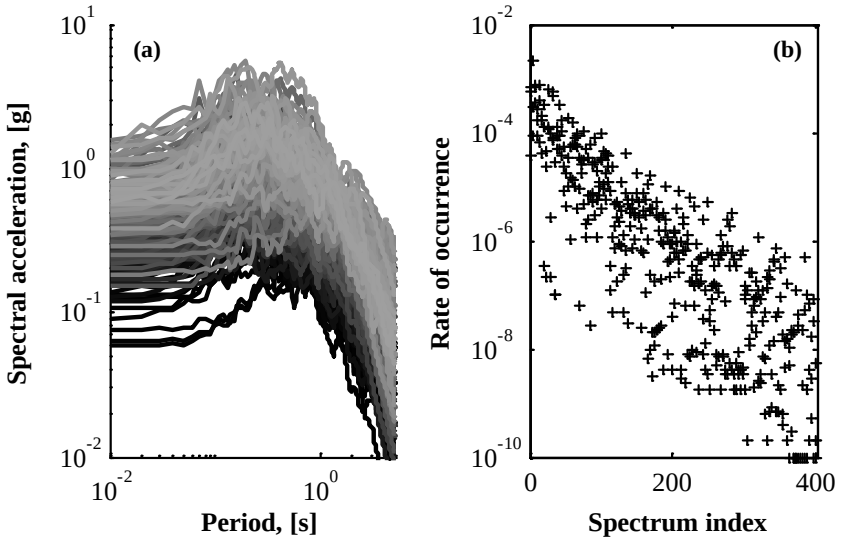

Figure 2 – Scenario spectra: (a) 402 scenario spectra (5% damped); (b) assigned rate of occurrence for each spectrum of the CSS

The hazard produced by the CSS can be estimated as

$$\nu(S_a(T) > z) = \sum_{i=1}^{\#recordings} Rate_{CS,i} H\left(S_{a,i}(T) - z\right) \quad (1)$$

where $S_{a,i}(T)$ is the spectral acceleration of the ith recording, z is a test level, and H is the Heavyside function (for example, H(x) =1 for x > 0 and H(x)=0 for x ≤ 0). For a given period, only the recordings with spectral

acceleration larger than test level z (for example, larger than certain value of Sa) will contribute to the hazard. In Figure 3, the hazard estimated with the CSS set is compared with that from a probabilistic hazard analysis (PSHA) for a site in northern California, United States. A good agreement is observed for hazard levels 10-5 to 10-2 (return periods of 100 to 100,000 years) for a wide range of structural periods, which demonstrates the hazard-consistency of the selected set.

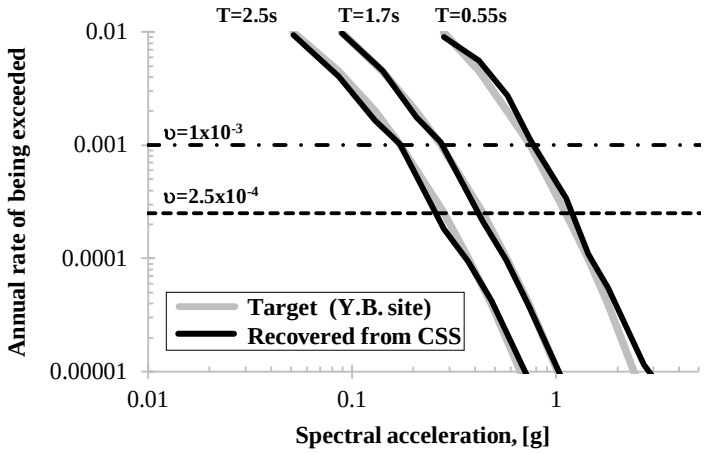

Figure 3 – Hazard curves at different periods recovered from the conditional scenario spectra.

2.1. EDP Risk Estimation from the CSS Set

A distributed plasticity force-based finite element model of a shear wall is constructed to present an example of the risk estimation methodology. The purpose is to test the implications of two modeling approaches with a hazard-consistent basis. Figure 4 presents the geometry of the wall in elevation, the details of the cross section reinforcement, as well as some modeling details. The wall is a modified version of that presented by Segura, et al. [6]. It has cross section of 7.5 ft [2.30 m] in length, with web and flange thickness of 12 in. [305 mm] was analysed for combined gravity and lateral seismic loads following ASCE-7 [7]. The special reinforced concrete shear wall of 84 ft [25.5 m] is the lateral load resisting system of 2100 ft^2 [190 m^2] of surrounding floor area. The expected axial load on the wall is $0.10A_g f'_c$; this was kept invariant for elastic and inelastic analyses purposes. For drift calculations, the effective inertia was set to 35% of the gross inertia. A response modification factor R = 5, and a deflection amplification factor C_d = 5, were selected. The concrete was assumed normal weight (γ_c = 150 lb/ft^3 [24 kN/m^3]) with nominal strength f'_c = 4.5 ksi [31 MPa]. The elastic modulus of the reinforced concrete structural elements was computed as $57000\sqrt{(f'_c)}$ [psi]. Reinforcing steel was assumed ASTM A706 with nominal yielding strength of f_y = 60 ksi [420 MPa]. Seismic load effects on the structural members were calculated by means of the Equivalent Lateral Force Analysis described in ASCE-7 [7]. The approximate period used for this purpose was estimated as $C_u T_a$ = 0.78s. Design base shear including response modification factor R was V = 315 kip [1390 kN] which is 13% of the seismic weight. Design maximum roof drift ratio was 0.98%. The maximum story drift ratio was kept below the 2% code limit. The design was performed in accordance with provisions for special structural walls in ACI 318-11 [8]. The special boundary element (SBE) on the stem has longitudinal steel ratio ρ_{SBE} = 2.9%, and transverse reinforcement ratio $A_{sh}/(sb_c)$ equal to 1.1% in the through-thickness direction of the wall. The flange side of the wall is reinforced as a SBE as well, with longitudinal steel ratio of 3.5%, which includes a protected area within the web. The longitudinal and transverse steel ratio of the web is $\rho_h = \rho_t$ = 0.0046, providing protection against shear failure in case the flexural capacity of the wall is reached.

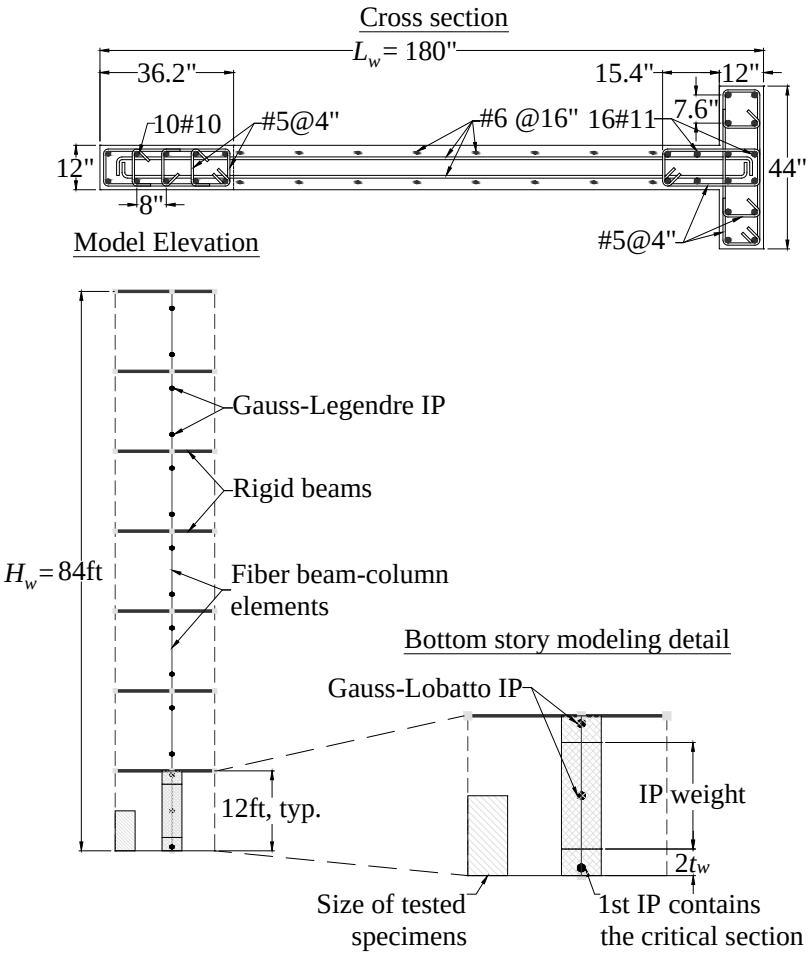

Figure 4 – Geometry, reinforcement and model of the T-wall studied (Note: 1" ≡ 1 in. = 25.4 mm; 1 ft = 304 mm).

2.2. Inelastic Modeling

Two models of the wall were constructed to show the effects of the softening response of the confined concrete in the boundary element region on the global displacement capacity. The one model that accounts for softening response is denoted SoM (soft-model). The other model does not degrade with large compressive strains and is denoted DuM (ductile-model). The cantilever wall geometry, material characteristics, and reinforcement were programmed in OpenSees [9]. The centerline of the elements representing the wall coincides with the centroid of the cross section and does not migrate with the neutral axis location. Shear deformations and nonlinear shear responses were not modeled. A force-based formulation was employed for the construction of the model. Two quadrature schemes were used: (i) Gauss-Lobatto with three integration points (IP) for the first story element, and (ii) Gauss-Legendre with 2IP for the rest. A physical interpretation often given to the weights of the quadrature rules used in the formulation of distributed plasticity elements is related to the spread of plasticity within the element. For softening behavior, it is expected that the inelastic demand over the element concentrates on a single integration point. In flexure, this result in high curvature demand at the section level, which in turns reduces the total deformation capacity of the system.

2.3. Materials

The post peak response of the confined concrete constitutive model implemented for the SoM is consistent with laboratory experiments on prismatic specimens in compression [10]. Recorded stress–strain relationships were estimated over gage lengths that approximate well the integration point length at the critical section of the wall model. This ensures that the local uniaxial strains obtained from the analysis adequately represent the physical phenomenon. The model implemented for the DuM has the same ascending branch as that of the SoM but the post peak response holds the strength in a ductile manner. Due to the material model capabilities in OpenSees, it is not expected that the DuM model reproduces the actual behavior at the section level for large compressive strains because it does not degrade in strength. Nevertheless, its responses serve the purpose of benchmarking for the SoM model. Figure 5 depicts the compression region of the constitutive model backbones for the SoM and DuM models. The longitudinal reinforcing steel stress-strain behavior was assumed to be bilinear with isotropic strain hardening.

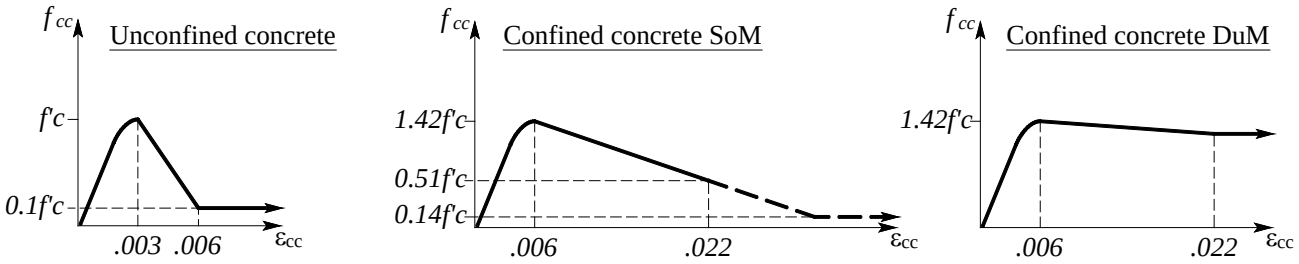

Figure 5 – Compression quadrant of the concrete models for nonlinear analysis.

2.4. SoM model EDP analysis

Response history analyses (RHA) of the SoM and the DuM models were performed with the CSS ground motion set. This section focuses on the results of the SoM model because are of most interest, given the softening nature of its response. The DuM model responses are used for comparison later. Figure 6 presents maximum roof drift ratio (RDR_{max}) versus spectral acceleration relationships. The spectral acceleration $S_a(T_1)$ is estimated at the fundamental period of the nonlinear model. Figure 6a depicts a scattergram of the data, showing increasing dispersion with increments of $S_a(T_1)$ and/or RDR_{max}. This indicates that elastic spectral acceleration might not be the best predictor for the response in mention. Nevertheless, the empirical data are binned by $S_a(T_1)$ level and lognormal fragility functions are estimated in Figure 6b using the methodology in [11]. The fragility functions are cumulative distribution functions defined by two parameter: the mean (μ_{Sa}) and the standard deviation of the natural logarithm of the intensity measure ($\sigma_{ln,Sa}$). As noted before, this is also a typical product of the Incremental Dynamic Analysis procedure. Three curves shown are for RDR_{max} > 0.5%, 2.0% and 4.0%. For RDR_{max} > 4%, the available empirical data are more scattered which impacts the slope of the fragility curve. This slope is a function of the variance estimator of the lognormal fit. According to the data in the fragilities, given that the spectral acceleration corresponding to the design value (S_a = 0.68 g) occurs at the Yerba Buena site, there is a 100%, 30% and 5% probability that the maximum roof drift ratio exceeds 0.5%, 2% and 4%, respectively. Per code definition, this acceleration value has a return period close to 475 years.

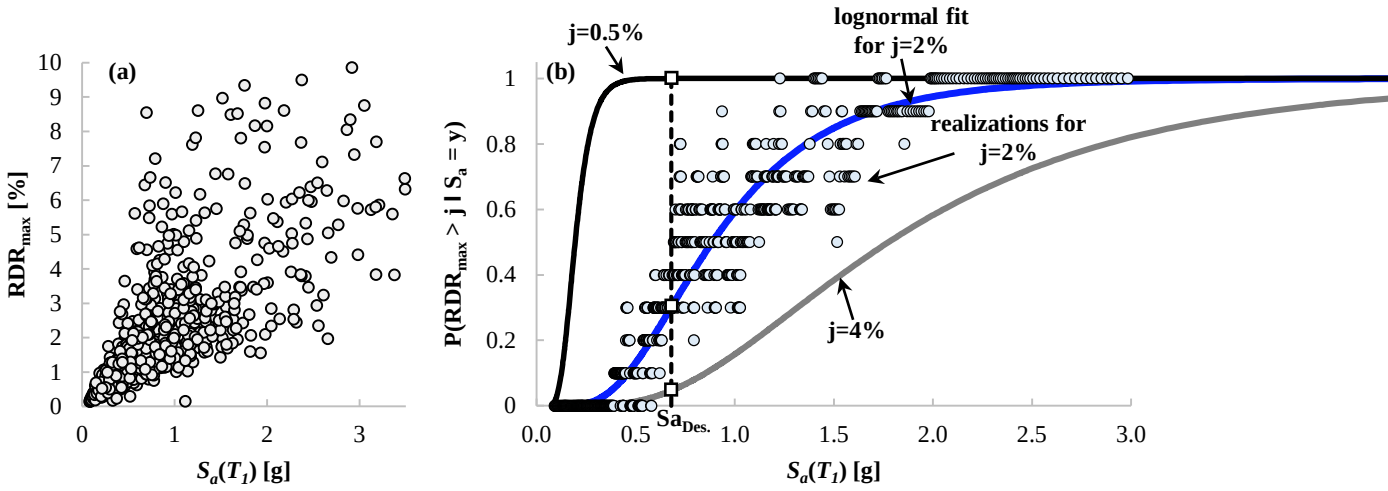

Figure 6 – Roof drift ratio versus spectral acceleration relationships: (a) scattergram of RDRmax and Sa(T1); (b) fragility curves for different levels of RDRmax.

2.5. Hazard-consistent structural response assessment with the CSS methodology

Figure 7 shows scatter plots relating two EDPs of interest with the corresponding rate of occurrence of each ground motion. A main assumption underlying the risk estimation methodology is that rates of occurrence are related to the spectral shape, and that ground motions with larger rate of occurrence produce smaller EDP values. This idea is supported by the fact that frequent ground motions are associated with lower intensity values. Figure 7a shows an example where a large rate is detected at a large RDRmax value. This will produce "jumps" in the corresponding risk curve, depending on the discretization level of the hazard. Again, this is another sign that elastic spectral accelerations might not be the best predictor of inelastic structural responses. A vector of parameters may be a better approach that would lead to smoother scaling with the ground motion levels. A discontinuity in the $\varepsilon_{c,max}$ cloud is apparent (Figure 7b) for strain values in excess of that at which the peak strength in the SBE is attained. This affects the EDP risk curve by flattening it, making the risk invariant to increasing levels of strain demand beyond the instability point.

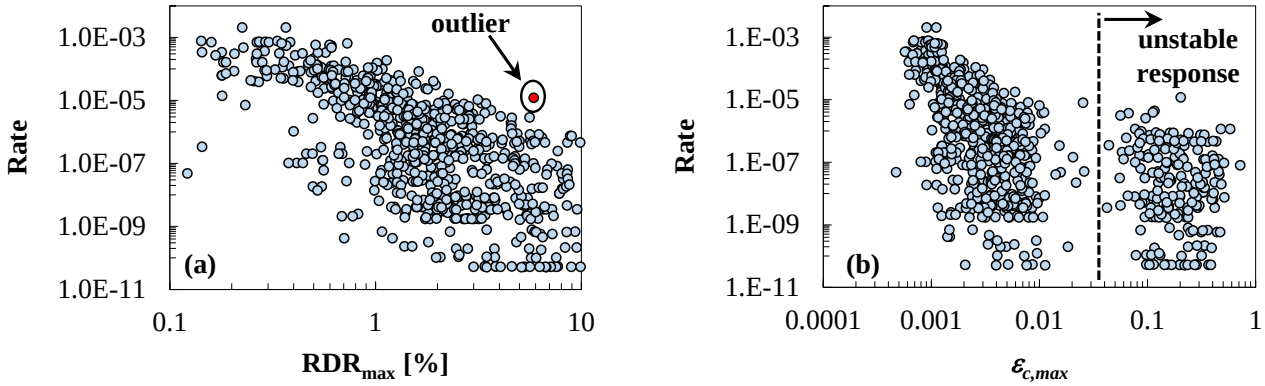

Figure 7 – Rate versus EDP level: (a) rates of occurrence for maximum roof drift ratio; (b) rates of occurrence for max-imum compressive strain in the stem SBE; (c) rates of occurrence for maximum tensile strain in the stem SBE.

The structural responses from the CSS, along with the assigned rates of each time series, allow direct estimation of the EDP risk using Equation 2:

$$\nu(EDP > d) = \sum_{i=1}^{\#recordings} Rate_{CS,i} H(EDP - d) \quad (2)$$

where $\nu_{EDP}(EDP > d)$ is the annual frequency with which demand level d is exceeded; and as before, $H(EDP - d)$ is either 1 or 0, per the Heaviside function H, depending on whether or not the EDP from time series *i* exceeds level *d*. The data reported in Figure 7 along with a similar dataset for the DuM model (not shown here for the sake of brevity) are used to estimate risk curves of the corresponding EDPs. It is worth recalling that the response of the DuM model is unrealistically ductile in the direction compressing the SBE in the stem, because of the non-degrading nature of its material models. Nevertheless, its responses are useful as an upper bound of proper behavior to contrast the result of the more realistic SoM model. The EDP risk of both models are presented in Figure 8 and Figure 9. The risk of maximum compressive strain $\varepsilon_{c,max}$ at the centroid of the SBE is shown in Figure 8. In this case, the SoM and DuM risk differ for strains larger than 0.003, which is associated with the onset of unconfined concrete crushing. Load redistribution due to loss of capacity of the cover generates additional stress demand in the adjacent material, consequently exacerbating the compressive strain demand on the confined concrete model. The ductile nature of the concrete model of the DuM model can take this additional demand without much loss of load carrying capacity, while the confined concrete model of the SoM may be pushed into the descending post peak slope. Two usable strain limits for the confined concrete are: $\widehat{\varepsilon_{cc100}}$ =0.006 and $\widehat{\varepsilon_{cc80}}$ =0.011, which define the peak strength, and that at which the confined concrete model has loss 20% of its capacity. These two values intersect the SoM risk curve at TR = 19,400 and 36,800 years, respectively. In general, compressive strain values in excess of 0.003 have a low associated risk, therefore, it is concluded that unstable flexural-compression behavior of the boundary element is not likely.

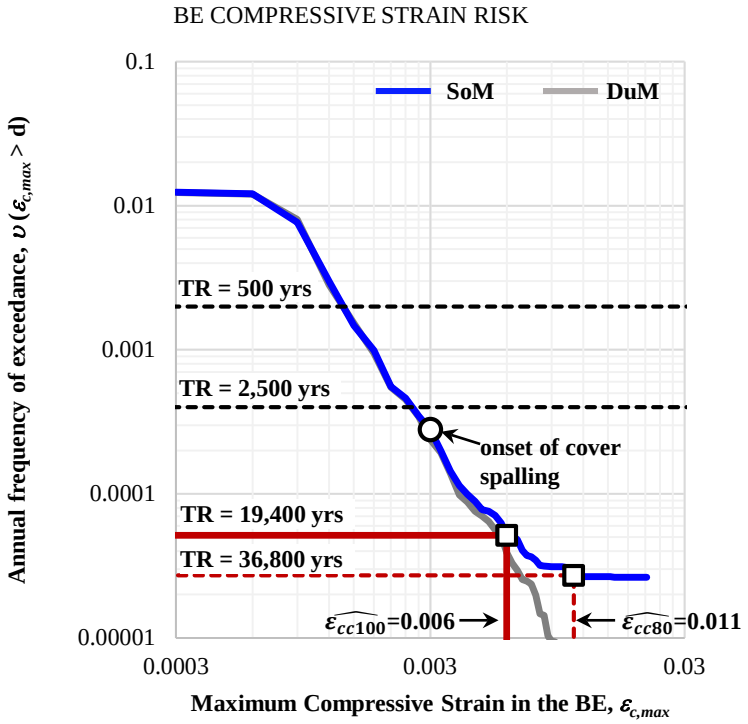

Figure 8 – Maximum SBE compressive strain risk for the SoM and DuM models.

Risk curves for the maximum roof drift ratio are presented in Figure 9. The return period for the design roof drift (approximately 1%) is 1,100 years, which contrasts with the 475 years return period accounted for by the code. This is explained by the fact that the elastic forces used for the estimation of the design drift where consistent with a lower structural period, as compared to the nonlinear model. At the same hazard level as that of the design, the nonlinear model was affected by lower spectral acceleration demand. Although both models differ in their constitutive relation of the confined concrete, the RDR_{max} risk curves only start to diverge at risk levels as low as 3×10^{-3} (TR = 3,500 years approximately). This risk level is consistent with that of the onset of cover crushing, and the same reason exposed above apply for the differences in displacement demand. The roof drift ratio at the MCE level of demand (for example, 2500 year) is below that producing cover spalling, therefore small damage in the system may be expected at that hazard level.

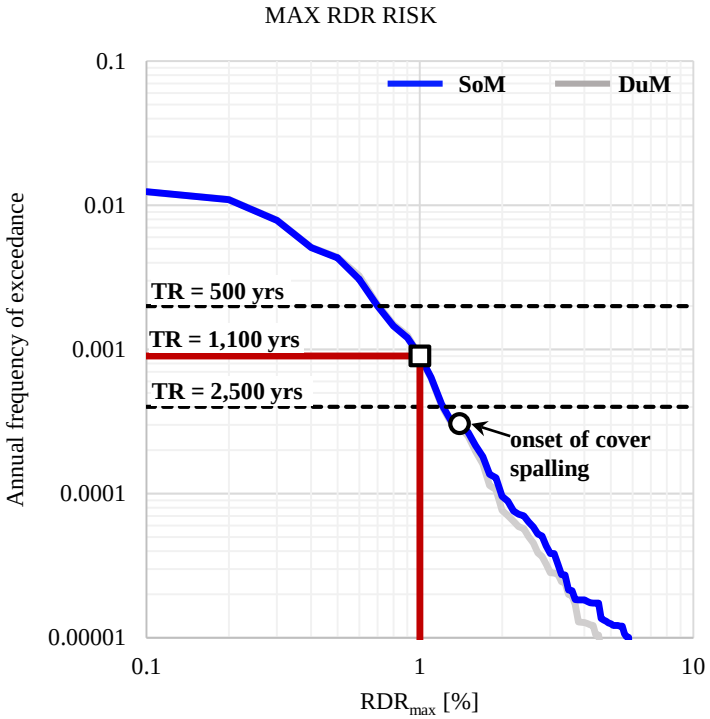

Figure 9 – Maximum roof drift ratio risk for the SoM and DuM models.

3. Final comments

A methodology to estimate the risk of several structural responses was presented. The methodology is based on the Conditional Scenario Spectra (CSS), which is a set of realistic earthquake spectra with assigned rates of occurrence that reproduce the hazard at a site. A numerical example of a code-compliant special structural wall is used to show the implementation of a hazard-consistent response assessment methodology. The single case example is utilized to describe the implication of the strain limits in the boundary region of element.

4. Copyrights

5. References

[1] Vamvatsikos, D., & Cornell, C. A. 2002. Incremental dynamic analysis, *Earthquake Engineering & Structural Dynamics*, 31(3), 491-514.

[2] Haindl, M., Hube, M., & Arteta, C. A. 2015. Seismic Performance Assessment of a Reinforced Concrete Shear Wall House, Proceedings of the VII Congreso Nacional de Ingeniería Sísmica, Bogotá, May 27-29, 2015.

[3] Lin, T., Harmsen, S. C., Baker, J. W., & Luco, N. 2013. Conditional Spectrum Computation Incorporating Multiple Causal Earthquakes and Ground-Motion Prediction Models, *Bulletin of the Seismological Society of America*, 103(2a), 1103-1116.

[4] Lin, T., Haselton, C. B., & Baker, J. W. 2013. Conditional spectrum-based ground motion selection. Part I: Hazard consistency for risk-based assessments, *Earthquake Engineering & Structural Dynamics*, 42(12), 1847-1865.

[5] Baker, J. W. 2011. Conditional Mean Spectrum: Tool for Ground-Motion Selection, *Journal of Structural Engineering*, 137(3), 322-331.

[6] Segura, C.L., Arteta, C.A., Wallace, J.W. & Moehle, J.P. 2016. Deformation capacity of thin reinforced concrete shear walls, Proceedings of the *New Zealand Society for Earthquake Engineering Conference, Christchurch, April 1-3 2016*.

[7] ASCE. (2010). Minimum Design Loads for Buildings and Other Structures (ASCE/SEI 7-10). Reston, VA: American Society of Civil Engineering/ Structural Engineering Institute.

[8] ACI-Committee-318. (2011). Building Code Requirements for Structural Concrete and Commentary (ACI 318-11). Farmington Hills, MI: American Concrete Institute.

[9] McKenna, F., Fenves, G. L., Scott, M. H., & Jeremic, B. (2000). Open system for earthquake engineering simulation (OpenSees) (Version 2.4.3.). Berkeley, CA: Pacific Earthquake Engineering Research Center, University of California.

[10] Arteta C.A., To, D.V. & Moehle, J.P. 2014. Experimental response of boundary elements of code-compliant reinforced concrete shear walls, *Proccedings of the 10th National Conference on Earthquake Engineering, Anchorage, July 21-25 2014*.

[11] Baker, J. W. (2015). "Efficient Analytical Fragility Function Fitting Using Dynamic Structural Analysis." Earthquake Spectra 31(1): 579-599.